

Probing a pseudoscalar at the LHC in light of $R(D^{(*)})$ and muon $g - 2$ excesses

Lei Wang¹, Jin Min Yang^{2,3}, Yang Zhang²

¹ Department of Physics, Yantai University, Yantai 264005, P. R. China

² CAS Key Laboratory of Theoretical Physics,

Institute of Theoretical Physics, Academia Sinica, Beijing 100190, P. R. China

³ School of Physics, University of Chinese Academy of Sciences, Beijing 100049, P. R. China

Abstract

We study the excesses of $R(D^{(*)})$ and muon $g - 2$ in the framework of a two-Higgs-doublet model with top quark flavor-changing neutral-current (FCNC) couplings. Considering the relevant theoretical and experimental constraints, we find that the $R(D^{(*)})$ and muon $g - 2$ excesses can be simultaneously explained in a parameter space allowed by the constraints. In such a parameter space the pseudoscalar (A) has a mass between 20 GeV and 150 GeV so that it can be produced from the top quark FCNC decay $t \rightarrow Ac$. Focusing on its dominant decay $A \rightarrow \tau\bar{\tau}$, we perform a detailed simulation on $pp \rightarrow t\bar{t} \rightarrow WbAc \rightarrow jjbc\tau\bar{\tau}$ and find that the 2σ upper limits from a data set of 30 (100) fb^{-1} at the 13 TeV LHC can mostly (entirely) exclude such a parameter space.

PACS numbers: 12.60.Fr, 14.80.Ec, 14.80.Bn

I. INTRODUCTION

Recently, the BaBar [1, 2], Belle [3, 4] and LHCb [5] collaborations have reported anomalies in the ratios

$$R(D^{(*)}) = \frac{\mathcal{B}(\bar{B} \rightarrow D^{(*)}\tau\bar{\nu}_\tau)}{\mathcal{B}(\bar{B} \rightarrow D^{(*)}\ell\bar{\nu}_\ell)}, \quad (1)$$

where $\ell = e, \mu$. The average values from the Heavy Flavor Average Group is [6]

$$R(D)_{\text{avg}} = 0.397 \pm 0.040 \pm 0.028, \quad (2)$$

$$R(D^*)_{\text{avg}} = 0.316 \pm 0.016 \pm 0.010. \quad (3)$$

Compared to the SM predictions

$$R(D)_{\text{SM}} = 0.300 \pm 0.008, \quad (4)$$

$$R(D^*)_{\text{SM}} = 0.252 \pm 0.003, \quad (5)$$

there is a discrepancy of 1.9σ for $R(D)$ and 3.3σ for $R(D^*)$. The anomalies have been studied in some specific new physics models [7–36], including the possibility of a charged Higgs boson [37–50].

On the other hand, the muon anomalous magnetic moment ($g - 2$) is a very precisely measured observable. The muon $g - 2$ anomaly has been a long-standing puzzle since the announcement by the E821 experiment in 2001 [51, 52]. There is an approximate 3σ discrepancy between the experimental value and the SM prediction [53–55]. The muon $g - 2$ anomaly can be simply explained in the two-Higgs-doublet model (2HDM) [56–72].

In this paper, we examine the $R(D^{(*)})$ and muon $g-2$ excesses in a 2HDM with the top quark flavor-changing neutral-current (FCNC) couplings. We consider various theoretical and experimental constraints from the precision electroweak data, the B -meson decays, the τ decays as well as the observables of the top quark and Higgs searches. In this model, the lepton Yukawa couplings can simultaneously affect $R(D^{(*)})$, muon $g-2$ and the lepton universality from τ decays, and thus these three observables have a strong correlation. The $R(D^{(*)})$ and muon $g-2$ excesses favor a light pseudoscalar with a large coupling to lepton and nonzero top FCNC couplings, which implies that the pseudoscalar can be produced from the top quark FCNC decay $t \rightarrow Ac$ and then dominantly decays in the mode $A \rightarrow \tau\bar{\tau}$. We will perform a detailed simulation on the signal $pp \rightarrow t\bar{t} \rightarrow WbAc \rightarrow jjbc\tau\bar{\tau}$ and the corresponding backgrounds at the LHC.

Our work is organized as follows. In Sec. II we recapitulate the 2HDM with the top quark FCNC couplings. In Sec. III we perform numerical calculations. In Sec. IV, we discuss the $R(D^{(*)})$ and muon g-2 excesses after imposing the relevant theoretical and experimental constraints, and then perform the simulations on $pp \rightarrow t\bar{t} \rightarrow WbAc \rightarrow jjbc\tau\bar{\tau}$. Finally, we give our conclusion in Sec. V.

II. TWO-HIGGS-DOUBLET MODEL WITH TOP QUARK FCNC COUPLINGS

The general Higgs potential is written as [73]

$$\begin{aligned} V = & m_{11}^2(\Phi_1^\dagger \Phi_1) + m_{22}^2(\Phi_2^\dagger \Phi_2) - \left[m_{12}^2(\Phi_1^\dagger \Phi_2 + \text{h.c.}) \right] \\ & + \frac{\lambda_1}{2}(\Phi_1^\dagger \Phi_1)^2 + \frac{\lambda_2}{2}(\Phi_2^\dagger \Phi_2)^2 + \lambda_3(\Phi_1^\dagger \Phi_1)(\Phi_2^\dagger \Phi_2) + \lambda_4(\Phi_1^\dagger \Phi_2)(\Phi_2^\dagger \Phi_1) \\ & + \left[\frac{\lambda_5}{2}(\Phi_1^\dagger \Phi_2)^2 + \text{h.c.} \right] + \left[\lambda_6(\Phi_1^\dagger \Phi_1)(\Phi_1^\dagger \Phi_2) + \text{h.c.} \right] \\ & + \left[\lambda_7(\Phi_2^\dagger \Phi_2)(\Phi_1^\dagger \Phi_2) + \text{h.c.} \right]. \end{aligned} \quad (6)$$

We focus on the CP-conserving model in which all λ_i and m_{12}^2 are real. We assume λ_6 and λ_7 are zero, and thus the Higgs potential has a softly broken Z_2 symmetry. The two complex scalar doublets have the hypercharge $Y = 1$:

$$\Phi_1 = \begin{pmatrix} \phi_1^+ \\ \frac{1}{\sqrt{2}}(v_1 + \phi_1^0 + ia_1) \end{pmatrix}, \quad \Phi_2 = \begin{pmatrix} \phi_2^+ \\ \frac{1}{\sqrt{2}}(v_2 + \phi_2^0 + ia_2) \end{pmatrix}, \quad (7)$$

where the electroweak vacuum expectation values (VEVs) $v^2 = v_1^2 + v_2^2 = (246 \text{ GeV})^2$, and the ratio of the two VEVs is defined as $\tan \beta = v_2/v_1$. After spontaneous electroweak symmetry breaking, there are five mass eigenstates: two neutral CP-even h and H , one neutral pseudoscalar A , and two charged scalars H^\pm .

The general Yukawa interactions in the physical basis are given as

$$\begin{aligned} -\mathcal{L} = & Y_{u1} \overline{Q}_L \tilde{\Phi}_1 u_R + Y_{d1} \overline{Q}_L \Phi_1 d_R + Y_{\ell 1} \overline{L}_L \Phi_1 e_R \\ & + Y_{u2} \overline{Q}_L \tilde{\Phi}_2 u_R + Y_{d2} \overline{Q}_L \Phi_2 d_R + Y_{\ell 2} \overline{L}_L \Phi_2 e_R + \text{h.c.}, \end{aligned} \quad (8)$$

where $Q_L^T = (u_L, d_L)$, $L_L^T = (\nu_L, l_L)$, $\tilde{\Phi}_{1,2} = i\tau_2 \Phi_{1,2}^*$, and $Y_{u1,2}$, $Y_{d1,2}$ and $Y_{\ell 1,2}$ are 3×3 matrices in family space.

To avoid the tree-level FCNC of the down-type quarks and leptons, we take the two Higgs doublet fields to have the aligned Yukawa coupling matrices [74, 75]:

$$Y_{\ell_1} = c_\ell \rho_\ell, \quad Y_{\ell_2} = s_\ell \rho_\ell, \quad (9)$$

$$Y_{d1} = c_d \rho_d, \quad Y_{d2} = s_d \rho_d, \quad (10)$$

where $c_d \equiv \cos \theta_d$, $s_d \equiv \sin \theta_d$, $c_\ell \equiv \cos \theta_\ell$, $s_\ell \equiv \sin \theta_\ell$, and ρ_d (ρ_ℓ) is the 3×3 matrix.

For the Yukawa coupling matrices of the up-type quarks, we take

$$X_{ii} = \frac{\sqrt{2}m_{ui}}{v}(s_\beta + c_\beta \kappa_u), \quad (11)$$

$$X_{ct} = \frac{\sqrt{2m_c m_t}}{v} c_\beta \lambda_{ct}, \quad (12)$$

$$X_{tc} = X_{ct}, \quad (13)$$

where $X = V_L Y_{u2} V_R^\dagger$, and V_L (V_R) is the unitary matrix which transforms the interaction eigenstates to the mass eigenstates for the left-handed (right-handed) up-type quark fields. We adopt the Cheng-Sher ansatz for X_{ct} and X_{tc} [76], and other non-diagonal matrix elements of X are taken as zero.

The Yukawa couplings of the neutral Higgs bosons are given as

$$\begin{aligned} y_{hf_if_i} &= \frac{m_{f_i}}{v} [\sin(\beta - \alpha) + \cos(\beta - \alpha)\kappa_f], \\ y_{Hf_if_i} &= \frac{m_{f_i}}{v} [\cos(\beta - \alpha) - \sin(\beta - \alpha)\kappa_f], \\ y_{Af_if_i} &= -i \frac{m_{f_i}}{v} \kappa_f \text{ (for u)}, \quad y_{Af_if_i} = i \frac{m_{f_i}}{v} \kappa_f \text{ (for d, } \ell\text{)}, \\ y_{hct} &= \cos(\beta - \alpha) \frac{\sqrt{m_c m_t}}{v} \lambda_{ct}, \quad y_{htc} = y_{hct}, \\ y_{Hct} &= -\sin(\beta - \alpha) \frac{\sqrt{m_c m_t}}{v} \lambda_{ct}, \quad y_{Htc} = y_{Hct}, \\ y_{Act} &= -i \frac{\sqrt{m_c m_t}}{v} \lambda_{ct}, \quad y_{Atc} = y_{Act}, \end{aligned} \quad (14)$$

where $\kappa_d \equiv -\tan(\beta - \theta_d)$ and $\kappa_\ell \equiv -\tan(\beta - \theta_\ell)$.

The Yukawa interactions of the charged Higgs are given as

$$\begin{aligned} \mathcal{L}_Y &= -\frac{\sqrt{2}}{v} H^+ \left\{ \bar{u}_i [\kappa_d (V_{CKM})_{ij} m_{dj} P_R - \kappa_u m_{ui} (V_{CKM})_{ij} P_L] d_j + \kappa_\ell \bar{\nu} m_\ell P_R \ell \right\} \\ &\quad - \frac{\sqrt{2m_c m_t}}{v} \lambda_{ct} H^+ [-\bar{u}_m (V_{CKM})_{nj} P_L d_j] + h.c., \end{aligned} \quad (15)$$

where $i, j = 1, 2, 3$, and $m, n = 2, 3$ with $m \neq n$.

The neutral Higgs boson couplings with the gauge bosons normalized to the SM are given by

$$y_V^h = \sin(\beta - \alpha), \quad y_V^H = \cos(\beta - \alpha), \quad (16)$$

where V denotes Z or W .

The non-diagonal matrix elements X_{ct} and X_{tc} lead to the top quark FCNC of h , H and A , and give additional contributions to the couplings of charged Higgs and top quark (charm quark), as shown in Eq. (14) and Eq. (15). In the exact alignment limit [77, 78], namely $\cos(\beta - \alpha) = 0$, from Eq. (14) and Eq. (16) we find that for h the couplings to the fermions and gauge bosons are same as in the SM, and the tree-level top quark FCNC couplings are absent. The heavy CP-even Higgs (H) has no couplings to the gauge bosons.

III. NUMERICAL CALCULATIONS

In our analysis we take the light CP-even Higgs boson h as the SM-like Higgs, $m_h = 125$ GeV. In order to avoid the constraints from the searches for the top quark FCNC of the SM-like Higgs, we take the exact alignment limit, namely $\sin(\beta - \alpha) = 1$. The muon $g - 2$ favors a light pseudoscalar with a large coupling to the lepton, and a sizable mass splitting between H and A . The precision electroweak data favors a small mass splitting of H and H^\pm . Therefore, we take

$$\begin{aligned} 20 \text{ GeV} &\leq m_A \leq 180 \text{ GeV}, & -150 \leq \kappa_\ell \leq -30, \\ 200 \text{ GeV} &\leq m_H \leq 700 \text{ GeV}, & 200 \text{ GeV} \leq m_{H^\pm} \leq 700 \text{ GeV}. \end{aligned} \quad (17)$$

In order to loose the constraints from the searches for $pp \rightarrow A$ (H) $\rightarrow \tau\bar{\tau}$ and the constraints from observables of down-type quarks, we take

$$\kappa_u = \kappa_d = -1/\kappa_\ell, \quad (18)$$

which is similar to the Yukawa couplings of the lepton-specific 2HDM. For a very large κ_ℓ , this choice is equivalent to assume κ_u and κ_d to be negligible.

The other free parameters are randomly scanned in the following ranges

$$0 < \lambda_{ct} < 30, \quad -(400 \text{ GeV})^2 \leq m_{12}^2 \leq (400 \text{ GeV})^2, \quad 0.1 \leq \tan \beta \leq 10. \quad (19)$$

Note that the $R(D^{(*)})$ excess favors opposite signs between λ_{ct} and κ_ℓ [42].

In our scan, we consider the following observables and constraints:

- (1) Theoretical constraints and precision electroweak data. We use 2HDMC [79, 80] to implement the theoretical constraints from the vacuum stability, unitarity and coupling-constant perturbativity, as well as the constraints from the oblique parameters (S , T , U) and $\delta\rho$.
- (2) The muon $g - 2$. At the one-loop level, the muon $g - 2$ is corrected by [56, 81, 82]

$$\Delta a_{\mu 1} = \frac{1}{8\pi^2} \sum_{\phi=h, H, A, H^\pm} |y_{\phi\mu\mu}|^2 r_{\phi\mu} f_\phi(r_{\phi\mu}), \quad (20)$$

where $r_{\phi\mu} = m_\mu^2/m_\phi^2$ and $y_{H^\pm\mu\mu} = y_{A\mu\mu}$. For $r_{\phi\mu} \ll 1$ we have

$$f_{h,H}(r) \simeq -\ln r - 7/6, \quad f_A(r) \simeq \ln r + 11/6, \quad f_{H^\pm}(r) \simeq -1/6. \quad (21)$$

The muon $g - 2$ can be also corrected by the two-loop Barr-Zee diagrams with the fermions loops and W loops. Using the well-known classical formulates [68, 83], the main contributions of two-loop Barr-Zee diagrams in the exact alignment limit are given as

$$\begin{aligned} \delta a_{\mu 2} = & -\frac{\alpha m_\mu}{4\pi^3 m_f} \sum_{\phi=h,H,A;f=t,b,\tau} N_f^c Q_f^2 y_{\phi\mu\mu} y_{\phi ff} F_\phi(x_{f\phi}) \\ & + \frac{\alpha m_\mu}{8\pi^3 v} \sum_{\phi=h} y_{\phi\mu\mu} g_{\phi WW} \left[3F_h(x_{W\phi}) + \frac{23}{4}F_A(x_{W\phi}) \right. \\ & \left. + \frac{3}{4}G(x_{W\phi}) + \frac{m_\phi^2}{2m_W^2} \{F_h(x_{W\phi}) - F_A(x_{W\phi})\} \right], \end{aligned} \quad (22)$$

where $x_{f\phi} = m_f^2/m_\phi^2$, $x_{W\phi} = m_W^2/m_\phi^2$, $g_{hWW} = 1$ and

$$F_\phi(y) = \frac{y}{2} \int_0^1 dx \frac{1-2x(1-x)}{x(1-x)-y} \log \frac{x(1-x)}{y} \quad (\text{for } \phi = h, H), \quad (23)$$

$$F_\phi(y) = \frac{y}{2} \int_0^1 dx \frac{1}{x(1-x)-y} \log \frac{x(1-x)}{y} \quad (\text{for } \phi = A), \quad (24)$$

$$G(y) = -\frac{y}{2} \int_0^1 dx \frac{1}{x(1-x)-y} \left[1 - \frac{y}{x(1-x)-y} \log \frac{x(1-x)}{y} \right]. \quad (25)$$

The difference between the SM value and the experimental value of muon $g - 2$ is

$$\delta a_\mu = (26.2 \pm 8.5) \times 10^{-10}. \quad (26)$$

- (3) Lepton universality from the τ decays. The current experimental results of the charged lepton universality from τ decays are given by [84]

$$\frac{g_\mu}{g_e} = 1.0018 \pm 0.0014, \quad \frac{g_\tau}{g_e} = 1.0029 \pm 0.0015, \quad \frac{g_\tau}{g_\mu} = 1.0001 \pm 0.0014, \quad (27)$$

where the first two values are from the fit to the leptonic decays of τ , and third value is from the fit to $\bar{\Gamma}(\tau \rightarrow e\nu\bar{\nu})/\bar{\Gamma}(\mu \rightarrow e\nu\bar{\nu})$, and $\bar{\Gamma}(\tau \rightarrow h\nu)/\bar{\Gamma}(h \rightarrow \mu\nu)$ with $h = K, \pi$ and $\bar{\Gamma}$ denoting the partial width normalized to its SM value. The ratio g_τ/g_e favors a positive correction to the SM value, which will impose strong constraints on the 2HDM, as shown in [65]. Since only two of the ratios in Eq. (27) are independent, in principle we may take g_μ/g_e and g_τ/g_μ to constrain the model.

In this model,

$$\left(\frac{g_\mu}{g_e}\right)^2 = \bar{\Gamma}(\tau \rightarrow \mu\nu\bar{\nu})/\bar{\Gamma}(\tau \rightarrow e\nu\bar{\nu}) \simeq 1 + \frac{z^2}{4} - \frac{2m_\mu}{m_\tau}z, \quad (28)$$

where $z = m_\mu m_\tau \kappa_\ell^2 / m_{H^\pm}^2$. The corrections are from the tree-level diagrams mediated by the charged Higgs. Since the one-loop effect applies equally to both tau decays, it does not give the correction to $\frac{g_\mu}{g_e}$.

Ignoring the electron mass, g_τ/g_μ is only corrected by the one-loop diagram mediated by the charged Higgs. The corrections to g_τ/g_μ is given by [65]

$$\left(\frac{g_\tau}{g_\mu}\right)^2 = \bar{\Gamma}(\tau \rightarrow e\nu\bar{\nu})/\bar{\Gamma}(\mu \rightarrow e\nu\bar{\nu}) \simeq 1 + 2\delta g, \quad (29)$$

where

$$\delta g = \frac{1}{16\pi^2} \left(\frac{m_\tau}{v} \kappa_\ell \right)^2 \left[1 + \frac{m_{H^\pm}^2 + m_A^2}{4(m_{H^\pm}^2 - m_A^2)} \log \frac{m_A^2}{m_{H^\pm}^2} + \frac{m_{H^\pm}^2 + m_H^2}{4(m_{H^\pm}^2 - m_H^2)} \log \frac{m_H^2}{m_{H^\pm}^2} \right]. \quad (30)$$

- (4) The measurements of $R(D^{(*)})$. The new four-fermion operators can be generated by exchanging the charged Higgs:

$$\mathcal{O}_{\text{SRL}}^q = (\bar{q}P_R b)(\bar{\tau}P_L \nu_\tau), \quad (31)$$

$$\mathcal{O}_{\text{SLL}}^q = (\bar{q}P_L b)(\bar{\tau}P_L \nu_\tau). \quad (32)$$

The corresponding tree-level Wilson coefficients are given by

$$C_{\text{SLL}}^c = \frac{2\sqrt{m_t m_c} m_\tau}{M_{H^\pm}^2 v^2} V_{tb} \lambda_{ct} \kappa_\ell, \quad C_{\text{SRL}}^c = -\frac{2m_b m_\tau}{M_{H^\pm}^2 v^2} V_{cb} \kappa_d \kappa_\ell, \quad (33)$$

which can give the contributions to $R(D^{(*)})$ [37–39, 46]

$$\begin{aligned} R(D) &= R_{\text{SM}}(D) \left(1 + 1.5 \text{Re} \left[\frac{C_{\text{SRL}}^c + C_{\text{SLL}}^c}{C_{\text{VLL}}^{c,\text{SM}}} \right] + 1.0 \left| \frac{C_{\text{SRL}}^c + C_{\text{SLL}}^c}{C_{\text{VLL}}^{c,\text{SM}}} \right|^2 \right), \\ R(D^*) &= R_{\text{SM}}(D^*) \left(1 + 0.12 \text{Re} \left[\frac{C_{\text{SRL}}^c - C_{\text{SLL}}^c}{C_{\text{VLL}}^{c,\text{SM}}} \right] + 0.05 \left| \frac{C_{\text{SRL}}^c - C_{\text{SLL}}^c}{C_{\text{VLL}}^{c,\text{SM}}} \right|^2 \right). \end{aligned} \quad (34)$$

Here $C_{\text{VLL}}^{c,\text{SM}}$ is the Wilson coefficient in the SM

$$C_{\text{VLL}}^{c,\text{SM}} = \frac{4G_F V_{cb}}{\sqrt{2}}. \quad (35)$$

- (5) B -meson decays. The non-diagonal matrix element X_{tc} can give additional contributions to the couplings of top quark and charged Higgs, which will correct Δm_{B_s} , Δm_{B_d} and $B \rightarrow X_s \gamma$ at the one-loop level:

$$H^+ \bar{t} s : -\frac{\sqrt{2}m_t}{v} V_{ts} \left(\kappa_u + \sqrt{\frac{m_c}{m_t}} \frac{V_{cs}}{V_{ts}} \lambda_{ct} \right) P_L + \frac{\sqrt{2}m_s}{v} V_{ts} \kappa_d P_R, \quad (36)$$

$$H^+ \bar{t} b : -\frac{\sqrt{2}m_t}{v} V_{tb} \left(\kappa_u + \sqrt{\frac{m_c}{m_t}} \frac{V_{cb}}{V_{tb}} \lambda_{ct} \right) P_L + \frac{\sqrt{2}m_b}{v} V_{tb} \kappa_d P_R. \quad (37)$$

The Δm_{B_s} , Δm_{B_d} and $B \rightarrow X_s \gamma$ are respectively calculated using the formulas in [85–87].

- (6) Higgs search experiments:

- (i) The non-observation of additional Higgs bosons. We employ **HiggsBounds-4.3.1** [88, 89] to implement the exclusion constraints from the neutral and charged Higgs searches at LEP, Tevatron and LHC at 95% confidence level.

Very recently, ATLAS reported the searches for a heavy charged Higgs in the single top quark associated production at the 13 TeV LHC with an integrated luminosity of 14.7 fb^{-1} for $H^\pm \rightarrow \tau \nu$ [90] and 13.2 fb^{-1} for $H^\pm \rightarrow tb$ [91]. The upper bounds of production cross section times $\text{Br}(H^\pm \rightarrow \tau \nu)$ are in the range of 2.0 to 0.008 pb for $m_{H^\pm} = 200\text{-}2000 \text{ GeV}$. The upper bounds of production cross section times $\text{Br}(H^\pm \rightarrow tb)$ are in the range of 1.37 and 0.18 pb for $m_{H^\pm} = 300\text{-}1000 \text{ GeV}$. In the model, the top quark FCNC of the charged Higgs can give additional contributions to the production of a charged Higgs boson in association with a top quark. Although the coupling of the charged Higgs and tau lepton is sizably enhanced, the decay $H^\pm \rightarrow AW^\pm$ is still an important mode.

- (ii) The global fit to the 125 GeV Higgs signal data. In the exact alignment limit, the SM-like Higgs couplings to the SM particles at tree-level are the same as the SM, which is favored by the 125 GeV Higgs signal data. For $m_A < 62.5 \text{ GeV}$, the mode $h \rightarrow AA$ can open and enhance the total width of h sizably, which will be strongly constrained by the 125 GeV Higgs data. We perform the χ^2 calculation

for the signal strengths in the $\mu_{ggF+tth}(Y)$ and $\mu_{VBF+Vh}(Y)$ with Y denoting the decay mode $\gamma\gamma$, ZZ , WW , $\tau\bar{\tau}$ and $b\bar{b}$,

$$\chi^2(Y) = \begin{pmatrix} \mu_{ggH+ttH}(Y) - \hat{\mu}_{ggH+ttH}(Y) \\ \mu_{VBF+VH}(Y) - \hat{\mu}_{VBF+VH}(Y) \end{pmatrix}^T \begin{pmatrix} a_Y & b_Y \\ b_Y & c_Y \end{pmatrix} \times \begin{pmatrix} \mu_{ggH+ttH}(Y) - \hat{\mu}_{ggH+ttH}(Y) \\ \mu_{VBF+VH}(Y) - \hat{\mu}_{VBF+VH}(Y) \end{pmatrix}, \quad (38)$$

where $\hat{\mu}_{ggH+ttH}(Y)$ and $\hat{\mu}_{VBF+VH}(Y)$ are the data best-fit values and a_Y , b_Y and c_Y are the parameters of the ellipse. These parameters are given by the combined ATLAS and CMS experiments [92]. We pay particular attention to the surviving samples with $\chi^2 - \chi^2_{\min} \leq 6.18$, where χ^2_{\min} denotes the minimum of χ^2 . These samples correspond to the 95.4% confidence level region in any two-dimension plane of the model parameters when explaining the Higgs data (corresponding to the 2σ range).

(7) Observables of the top quark:

- (i) The total width of the top quark. There is no decay mode $t \rightarrow hc$ in the exact alignment limit. For $m_A < m_t$, the mode $t \rightarrow Ac$ will open and enhance the total width of the top quark. The measurement value of the total top width is $\Gamma_t^{exp} = 1.36 \pm 0.02^{+0.14}_{-0.11}$ GeV from the CMS collaboration [93].
- (ii) Same-sign top pair production at the LHC. The same-sign top pair can be produced at the LHC via the $c\bar{c} \rightarrow t\bar{t}$ process with the t -channel exchange of A and H . From the searches for the same-sign dileptons and b-jets at the 8 TeV LHC with an integrated luminosity of 20.3 fb^{-1} [94], ATLAS gave an upper bound of 62 fb.

Note that the observables of the top quark, B -meson decays and the searches for the heavy charged Higgs at the 13 TeV LHC are all sensitive to the FCNC of top quark, namely the parameter λ_{ct} . For convenience, we use "Top-FCNC-Constraints" to denote these constraints in the following sections. We perform **MG5@NLO** [95] to calculate the cross section of $pp \rightarrow tt$ at the 8 TeV LHC and $\sigma(pp \rightarrow tH^\pm) \times Br(H^\pm \rightarrow \tau\nu, tb)$ at the 13 TeV LHC. In fact, our calculations show that the searches for the same-sign top pair production at the 8 TeV LHC

and the charged Higgs at the 13 TeV LHC can hardly give further constraints on the model after imposed the constraints from the B -meson decays, top width, muon $g - 2$, $R(D^{(*)})$, τ decays, precision electroweak data and theoretical constraints.

IV. RESULTS AND DISCUSSIONS

A. Explanation for $R(D^{(*)})$ and muon $g - 2$

In Fig. 1, we project the surviving samples on the planes of λ_{ct} versus m_{H^\pm} , κ_ℓ versus m_{H^\pm} and κ_ℓ versus λ_{ct} . Without the "Top-FCNC-Constraints", the λ_{ct} and $|\kappa_\ell|$ increase with the charged Higgs mass, and $|\kappa_\ell|$ tends to decrease with the increasing of λ_{ct} . These features are mainly determined by $R(D^{(*)})$ since the product $\lambda_{ct}\kappa_\ell/m_{H^\pm}^2$ in the Wilson coefficient C_{SLL}^c can affect $R(D^{(*)})$ (see Eq. (33) and Eq. (34)). In addition, the observables of the lepton universality from τ decays favor $|\kappa_\ell|$ to increase with the charged Higgs mass mainly due to the factor $\kappa_\ell^2/m_{H^\pm}^2$ in the correction terms of g_μ/g_e (see Eq. (28)).

After imposing the "Top-FCNC-Constraints", a large part of the parameter space is excluded, and λ_{ct} and m_{H^\pm} are directly constrained. For a given m_{H^\pm} , λ_{ct} will be imposed an upper bound by the "Top-FCNC-Constraints" and a lower bound by $R(D^{(*)})$. Once m_{H^\pm} and the upper bound of λ_{ct} are given, $R(D^{(*)})$ will impose a lower bound on $|\kappa_\ell|$. In addition, the lepton universality from τ decays will give an upper bound on $|\kappa_\ell|$ for a given m_{H^\pm} . For example, $3.0 < \lambda_{ct} < 4.5$ and $90 < |\kappa_\ell| < 125$ for $m_{H^\pm} = 400$ GeV. After imposing "Top-FCNC-Constraints", λ_{ct} and $|\kappa_\ell|$ increase with the charged Higgs mass, and $|\kappa_\ell|$ tends to increase with λ_{ct} . For $200 \text{ GeV} < m_{H^\pm} < 620 \text{ GeV}$, λ_{ct} and $|\kappa_\ell|$ are respectively required to be in the ranges of $1.5 \sim 6.5$ and $60 \sim 150$.

In Fig. 2, we project the surviving samples on the planes of κ_ℓ versus m_A and λ_{ct} versus m_A . The left panel shows that $|\kappa_\ell|$ is sensitive to m_A , and increases with m_A . These features are mainly determined by the muon $g - 2$ which is given the dominantly positive contributions by the pseudoscalar via the two-loop Barr-Zee diagrams. For $m_A > 150$ GeV, $|\kappa_\ell|$ is required to be larger than 150, which potentially leads to a problem with the perturbativity of the lepton Yukawa coupling. For $m_A = 20$ GeV, $|\kappa_\ell|$ is required to be larger than 60 after imposing "Top-FCNC-Constraints". Compared to the region of $m_A > 62.5$ GeV, there are relatively few surviving samples in the region of $m_A < 62.5$ GeV. For m_A smaller than

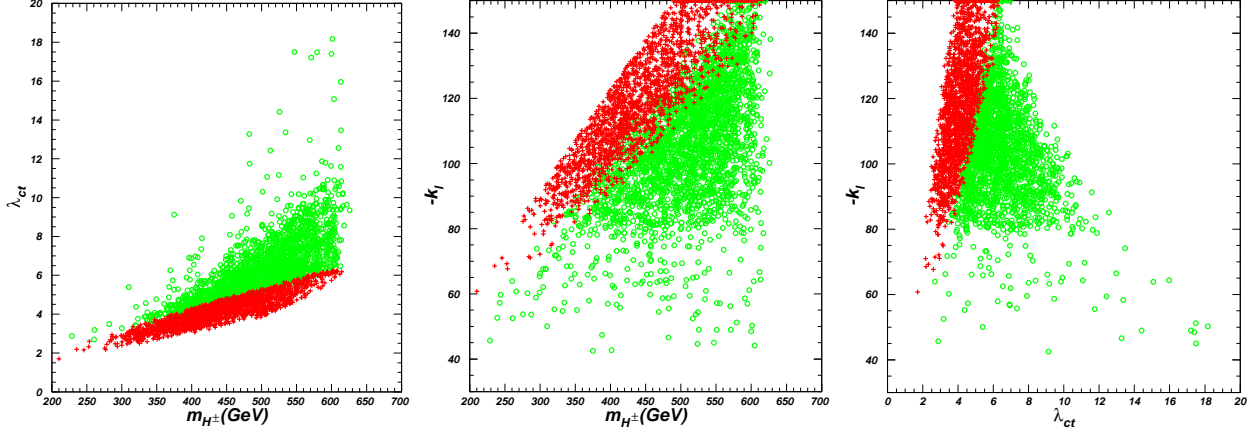


FIG. 1: The surviving samples projected on the planes of λ_{ct} versus m_{H^\pm} , κ_ℓ versus m_{H^\pm} and κ_ℓ versus λ_{ct} . All the points are allowed by the constraints of the muon $g - 2$, $R(D^{(*)})$, the theoretical constraints, the precision electroweak data, the τ decays, the exclusion limits of Higgs bosons and the 125 GeV Higgs data. The circles (green) and pluses (red) are respectively excluded and allowed by the "Top-FCNC-Constraints".

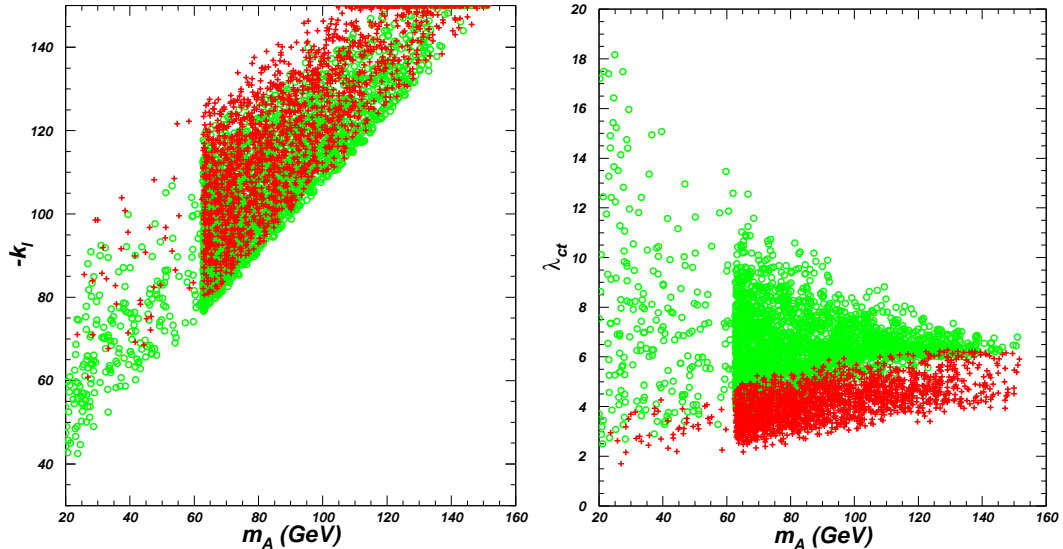


FIG. 2: Same as Fig. 1, but showing κ_ℓ versus m_A and λ_{ct} versus m_A .

the half of the SM-like Higgs mass, the decay mode $h \rightarrow AA$ will open and enhance the total width of the SM-like Higgs. Therefore, the data of the 125 GeV Higgs can give strong constraints on the parameter space.

The right panel of Fig. 2 shows that the surviving samples favor a large λ_{ct} for a large m_A to after imposing the "Top-FCNC-Constraints". Since the contributions of A and H to muon $g - 2$ canceled, a large mass splitting of A and H is required to explain the muon

$g - 2$. In addition, the precision electroweak data favor a small mass splitting of H and H^\pm . Therefore, the muon $g - 2$ favors a large m_{H^\pm} for a large m_A , and further a large m_{H^\pm} tends to require a large λ_{ct} due to the $R(D^{(*)})$ excess and "Top-FCNC-Constraints".

Note that flipping the signs of λ_{ct} and κ_ℓ does not change the results in this paper. As seen from section III, the muon $g - 2$ and the observables of lepton universality do not depend on the sign of κ_ℓ . $R(D^{(*)})$ depends on the sign of the product of $\lambda_{ct}\kappa_\ell$. When flipping the signs of λ_{ct} and κ_ℓ , the sign of the charged Higgs coupling of top quark will be flipped and the absolute value remains unchanged due to $\kappa_u = \kappa_d = -\kappa_\ell$, which does not change the results of B -meson decays.

B. Simulation on $pp \rightarrow t\bar{t} \rightarrow WbAc \rightarrow jjbc\tau\bar{\tau}$

As seen from the preceding section, after imposing the relevant theoretical and experimental constraints, the muon $g - 2$ and $R(D^{(*)})$ excesses can be simultaneously explained in the parameter space:

$$20 \text{ GeV} < m_A < 150 \text{ GeV}, \quad 200 \text{ GeV} < m_H \text{ } (m_{H^\pm}) < 620 \text{ GeV}, \\ -150 < \kappa_\ell < -60, \quad \kappa_u = \kappa_d = -1/\kappa_\ell, \quad 1.5 < \lambda_{ct} < 6.5. \quad (39)$$

In such a parameter space, the pseudoscalar can be produced via the QCD process $pp \rightarrow t\bar{t}$ followed by the decay $t \rightarrow Ac$, and then dominantly decays into $\tau\bar{\tau}$.

In the parameter space shown in Eq. (39), the decay modes $A \rightarrow HZ$, $A \rightarrow H^\pm W^\mp$ and $A \rightarrow hZ$ are kinematically forbidden, and $A \rightarrow hZ$ is also absent in the exact alignment limit. The pseudoscalar will dominantly decay into $\tau\bar{\tau}$, $Br(A \rightarrow \tau\bar{\tau}) \simeq 99.65\%$ and $Br(A \rightarrow \mu\bar{\mu}) \simeq 0.35\%$, which are not sensitive to $|\kappa_\ell|$ in the range of 60 to 150. Therefore, here the cross section $pp \rightarrow t\bar{t}$ times $Br(t \rightarrow Ac \rightarrow \tau\bar{\tau}c)$ is only sensitive to m_A and λ_{ct} . Besides, since the cross sections of $pp \rightarrow A$ and $pp \rightarrow At\bar{t}$ are sizably suppressed by κ_u^2 , the $pp \rightarrow t\bar{t} \rightarrow WbAc$ production process becomes more important.

Now we perform detailed simulations on the signal and backgrounds at the 13 TeV LHC. We consider the top quark pair production where one decays to $(W \rightarrow jj) + b$ and the other decays to $(A \rightarrow \tau\bar{\tau}) + c$. The major SM background processes to this signal are $t\bar{t}$, $tW+jets$, $tZ+jets$ and $Zb\bar{b}+jets$. Other backgrounds, such as the multi-jets, can be significantly reduced by requiring one b-tagged jet, two τ -tagged jets.

The model file of the 2HDM is generated by **FeynRules** [96]. Both the signal and background processes are generated with **MG5@NLO** [95], using **PYTHIA** for showering and hadronization [97], **TAUOLA** for τ lepton decay [98]. The fast simulations of the detector and trigger are performed by **Delphes3.3.0** [99], including **Fastjet3** for jet clustering [100].

We identify the lepton candidates by requiring them to have $p_T > 15$ GeV and $|\eta| < 2.5$. The anti-kt algorithm is employed to reconstruct the jets with a radius parameter $R = 0.4$ [101], and the jets are required to have $p_T > 20$ GeV and $|\eta| < 2.5$. We assume an average b-tagging efficiency of 70% for real b-jets, with misidentification efficiency of 10%, 4% and 0.2% for c-jets, τ -jets and jets initiated by light quarks or gluons respectively. We use the medium hadronic τ identification criteria with an efficiency of about 55% [102]. In order to suppress multi-jet backgrounds, we also require that the jets separated by $R < 0.2$ from the τ -tagged jet are removed.

According to the signal topology, we consider a final state of more than six jets including exactly two tau-tagged jets, one or two b-tagged jets, with missing transverse momentum $E_T^{miss} > 20$ GeV. Events with electrons or muons are vetoed. For event selection we require that the E_T^{miss} centrality C_{miss} is greater than zero [103]:

$$C_{miss} = \frac{x + y}{\sqrt{x^2 + y^2}}, \quad x = \frac{\sin(\phi_{miss} - \phi_{\tau 1})}{\sin(\phi_{\tau 2} - \phi_{\tau 1})}, \quad y = \frac{\sin(\phi_{\tau 2} - \phi_{miss})}{\sin(\phi_{\tau 2} - \phi_{\tau 1})}, \quad (40)$$

where ϕ_{miss} is the azimuthal angle of E_T^{miss} , and $\phi_{\tau 1,2}$ are the azimuthal angle of the two tau-tagged jets in the transverse plane.

To suppress the backgrounds, we reconstruct the kinematics of the top quarks from the corresponding decay particles. Firstly, because of the presence of the neutrino in τ hadronic decay, we use the collinear approximation technique to determine the 4-momenta of neutrino [104], which is based on two assumptions: the neutrinos from each τ are collinear with the corresponding visible τ decay products and E_T^{miss} is only due to neutrinos. For our signal events, there is no other E_T^{miss} contribution and the τ leptons are from the cascade decay of the top quark which can be boosted depending on m_A . The invisible momentum of neutrino in each τ decay is determined by

$$\begin{aligned} E_T^{miss} \cos \phi_{miss} &= p_{mis1} \sin \theta_{vis1} \cos \phi_{vis1} + p_{mis2} \sin \theta_{vis2} \cos \phi_{vis2}, \\ E_T^{miss} \sin \phi_{miss} &= p_{mis1} \sin \theta_{vis1} \sin \phi_{vis1} + p_{mis2} \sin \theta_{vis2} \sin \phi_{vis2}. \end{aligned} \quad (41)$$

where ϕ_{miss} is the azimuthal angle of E_T^{miss} , $\theta_{vis1,2}$ and $\phi_{vis1,2}$ are the polar and azimuthal angles of the τ jets, and p_{mis1} and p_{mis2} are the invisible momentum of τ decay. Then one

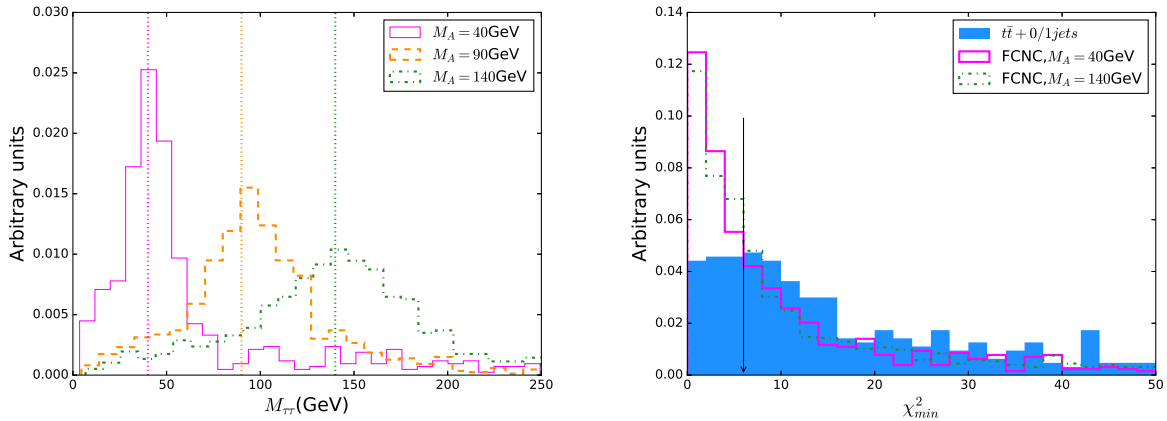


FIG. 3: The left panel is the distributions of the reconstructed mass $M_{\tau\tau}$ for the signal events with $M_A = 40$ GeV (solid line), $M_A = 90$ GeV (dashed line) and $M_A = 140$ GeV (dash-dotted line). The right panel is the distributions of χ^2_{min} for the signal events with $M_A = 40$ GeV (solid line) and $M_A = 140$ GeV (dash-dotted line) and for the main background $t\bar{t} + 0/1$ jet events (bins). The arrow represents the cut used in the event selection. All distributions are normalized to the unit area.

can obtain the invariant mass of the two τ leptons $M_{\tau\tau}$ and compare with the mass of the pseudoscalar A . In the left panel of Fig. 3, we show some examples for the distributions of $M_{\tau\tau}$ for the signal events with $M_A = 40$ GeV, 90 GeV and 140 GeV. One can see that this technique is more effective for a small m_A .

Since the mass of the pseudoscalar A is unknown, we use the reconstruct mass of top quark $m_{j_c\tau\tau}$ instead of $M_{\tau\tau}$. Together with the reconstructed masses of the SM decay of top quark and the W boson, $m_{j_b j_1 j_2}$ and $m_{j_1 j_2}$, we define a χ^2 function as

$$\chi^2 = \frac{(m_{j_c\tau\tau} - m_{FCNC})^2}{\sigma_{FCNC}^2} + \frac{(m_{j_b j_1 j_2} - m_t)^2}{\sigma_{SM}^2} + \frac{(m_{j_1 j_2} - m_W)^2}{\sigma_W^2}, \quad (42)$$

where $m_{FCNC} = 153$ GeV, $m_t = 173$ GeV, $\sigma_{FCNC} = 20$ GeV, $\sigma_{SM} = 20$ GeV, $m_W = 82$ GeV and $\sigma_W = 15$ GeV taken from [103, 105]. As we keep the events containing two b-tagged jets in which one of them is misidentified for the charm quark from the $t \rightarrow Ac$, the assignment of each jet to the reconstruct masses is dependent on the number of b-tagged jets. For the events involving two b-tagged jets, any b-tagged jet can be assigned to j_c and j_b , while j_1 and j_2 correspond to the leading two light-flavor jets. For events containing one b-tagged jet, the b-tagged jet is referred to j_b , j_c is chosen from the leading three light-flavor jets, and the other two jets in the leading three light-flavor jets act as j_1, j_2 . From all the combinations,

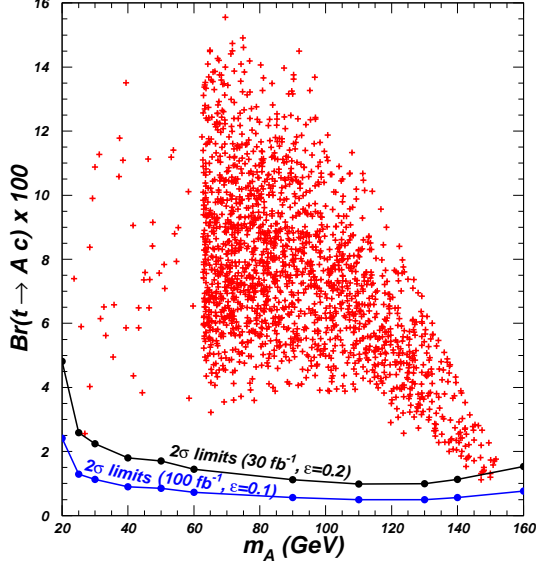


FIG. 4: The 2σ upper limits on $\text{Br}(t \rightarrow Ac)$ as functions of m_A for a data set of 30 fb^{-1} and 100 fb^{-1} at the 13 TeV LHC. All the samples satisfy the relevant constraints and can simultaneously explain the muon g-2 and $R(D^{(*)})$ excesses.

the one with the minimum χ^2_{min} is chosen, and then we require $\chi^2_{min} < 6$ according to the distributions of χ^2_{min} for signal and background events as shown in Fig 3.

After imposing the above selection conditions, the cross section of $t\bar{t}$ at the 13 TeV LHC is reduced to 61.3 fb , while $Z + b\bar{b}/c\bar{c}$ and tZ are reduced to 0.12 fb and 0.03 fb , respectively. Then we calculate the signal significance with simplified definition,

$$\mathcal{S} = \frac{n_s}{\sqrt{n_b + (\varepsilon n_b)^2}}, \quad (43)$$

where n_s and n_b are the expected numbers of the signal and background event, and ε is the relative systematic uncertainty which we conservatively take 20% and 10% for a data set of 30 fb^{-1} and 100 fb^{-1} at the 13 TeV LHC in our analysis. In Fig. 4 we show the results in plane of m_A and $\text{Br}(t \rightarrow Ac)$. All the samples in Fig. 4 satisfy the relevant constraints and can explain the muon $g - 2$ and $R(D^{(*)})$ excesses simultaneously. Depending on m_A , the branching ratio of $t \rightarrow Ac$ is required to above 1% and below 16%. The 2σ upper limits from a data set of 30 fb^{-1} at the 13 TeV LHC can exclude almost all the samples, and a few samples can survive only when m_A approaches to 150 GeV or 20 GeV. However, the 2σ upper limits from a data set of 100 fb^{-1} at 13 TeV LHC can exclude all the samples.

V. CONCLUSION

In the framework of a two-Higgs-doublet model with top quark FCNC couplings, we examined the excesses of $R(D^{(*)})$ and muon $g - 2$ by imposing the relevant theoretical and experimental constraints from the precision electroweak data, B -meson decays, τ decays, the observables of top quark and Higgs searches. In this model the coupling κ_ℓ can simultaneously affect $R(D^{(*)})$, the muon $g - 2$ and the lepton universality from τ decays, and thus these three observables have a strong correlation.

We found that the $R(D^{(*)})$ and muon $g - 2$ excesses can be simultaneously explained in the parameter space allowed by the relevant constraints. In such a parameter space, the pseudoscalar is between 20 GeV and 150 GeV so that it can be produced from the top quark FCNC decay $t \rightarrow Ac$ and then dominantly decays into $\tau\bar{\tau}$. We performed a detailed simulation on the signal $pp \rightarrow t\bar{t} \rightarrow WbAc \rightarrow jjbc\tau\bar{\tau}$ and the corresponding backgrounds, and found that the 2σ upper limits from a data set of 30 (100) fb^{-1} at the 13 TeV LHC can mostly (totally) exclude such a parameter space.

Acknowledgment

We thank Xin-Qiang Li, Ying Li and Zhi-Tian Zou for discussions. This work is supported by the National Natural Science Foundation of China under grant Nos. 11575152, 11275245, 11135003, by the CAS Center for Excellence in Particle Physics (CCEPP) and by the CAS Key Research Program of Frontier Sciences.

-
- [1] BaBar Collaboration, J. P. Lees et al., Phys. Rev. Lett. **109** (2012) 101802.
 - [2] BaBar Collaboration, J. P. Lees et al., Phys. Rev. D **88** (2013) 072012.
 - [3] Belle Collaboration, M. Huschle et al., Phys. Rev. D **92** (2015) 072014.
 - [4] Belle Collaboration, A. Abdesselam et al., arXiv:1603.06711.
 - [5] Collaboration, R. Aaij et al., Phys. Rev. Lett. **115** (2015) 111803 [Addendum: Phys. Rev. Lett. **115** (2015) 159901].
 - [6] Heavy Flavor Averaging Group (HFAG) Collaboration. Online results at http://www.slac.stanford.edu/xorg/hfag/semi/winter16/winter16_dtaunu.html.

- [7] M. Freytsis, Z. Ligeti, and J. T. Ruderman, Phys. Rev. D **92** (2015) 054018.
- [8] L. Calibbi, A. Crivellin, and T. Ota, Phys. Rev. Lett. **115** (2015) 181801.
- [9] F. F. Deppisch, S. Kulkarni, H. Päs, and E. Schumacher, Phys. Rev. D **94** (2016) 013003.
- [10] B. Dumont, K. Nishiwaki, and R. Watanabe, Phys. Rev. D **94** (2016) 034001.
- [11] I. Doršner, S. Fajfer, A. Greljo, J. F. Kamenik, and N. Košnik, Phys. Rept. **641** (2016) 1.
- [12] Y. Sakaki, M. Tanaka, A. Tayduganov, and R. Watanabe, Phys. Rev. D **91** (2015) 114028.
- [13] M. Bauer and M. Neubert, Phys. Rev. Lett. **116** (2016) 141802.
- [14] S. Fajfer and N. Košnik, Phys. Lett. B **755** (2016) 270-274.
- [15] S. Sahoo and R. Mohanta, Phys. Rev. D **93** (2016) 114001.
- [16] R. Barbieri, G. Isidori, A. Pattori, and F. Senia, Eur. Phys. Jour. C **76** (2016) 67.
- [17] Y. Sakaki, M. Tanaka, A. Tayduganov, and R. Watanabe, Phys. Rev. D **88** (2013) 094012.
- [18] S. M. Boucenna, A. Celis, J. Fuentes-Martin, A. Vicente, and J. Virto, Phys. Lett. B **760** (2016) 214.
- [19] C. Hati, G. Kumar, and N. Mahajan, JHEP **01** (2016) 117.
- [20] A. Greljo, G. Isidori, and D. Marzocca, JHEP **07** (2015) 142.
- [21] D. Das, C. Hati, G. Kumar, and N. Mahajan, arXiv:1605.06313.
- [22] J. Zhu, H.-M. Gan, R.-M. Wang, Y.-Y. Fan, Q. Chang, and Y.-G. Xu, Phys. Rev. D **93** (2016) 094023.
- [23] N. G. Deshpande and A. Menon, JHEP **01** (2013) 025.
- [24] X.-Q. Li, Y.-D. Yang, X. Zhang, arXiv:1605.09308.
- [25] N. G. Deshpande, X.-G. He, arXiv:1608.04817.
- [26] B. Bhattacharya, A. Datta, J.-P. Guevin, D. London, R. Watanabe, arXiv:1609.09078.
- [27] Z. Ligeti, M. Papucci, D. J. Robinson, arXiv:1610.02045.
- [28] D. Bardhan, P. Byakti, D. Ghosh, arXiv:1610.03038.
- [29] C. S. Kim, G. Lopez-Castro, S. L. Tostado, A. Vicente, arXiv:1610.04190.
- [30] D. Becirevic, S. Fajfer, N. Kosnik, O. Sumensari, arXiv:1608.08501.
- [31] A. K. Alok, D. Kumar, S. Kumbhakar, S. Sankar, arXiv:1606.03164.
- [32] S. Sahoo, R. Mohanta, A. K. Giri, arXiv:1609.04367.
- [33] A. Datta, M. Duraisamy, D. Ghosh, Phys. Rev. D **86** (2012) 034027.
- [34] B. Bhattacharya, A. Datta, D. London, S. Shivashankara, Phys. Lett. B **742** (2015) 370-374.
- [35] M. Duraisamy, P. Sharma, A. Datta, Phys. Rev. D **90** (2014) 074013.

- [36] M. Duraisamy, A. Datta, JHEP **1309** (2013) 059.
- [37] A. Crivellin, C. Greub and A. Kokulu, Phys. Rev. D **86** (2012) 054014.
- [38] A. G. Akeroyd and S. Recksiegel, J. Phys. G **29** (2003) 2311.
- [39] S. Fajfer, J. F. Kamenik and I. Nisandzic, Phys. Rev. D **85** (2012) 094025.
- [40] A. Celis, M. Jung, X.-Q. Li, and A. Pich, JHEP **01** (2013) 054.
- [41] J. M. Cline, Phys. Rev. D **93** (2016) 075017.
- [42] C. S. Kim, Y. W. Yoon, and X.-B. Yuan, JHEP **12** (2015) 038.
- [43] A. Crivellin, J. Heeck, and P. Stoffer, Phys. Rev. Lett. **116** (2016) 081801.
- [44] D. S. Hwang, arXiv:1504.06933.
- [45] A. Crivellin, A. Kokulu, and C. Greub, Phys. Rev. D **87** (2013) 094031.
- [46] Y. Sakaki and H. Tanaka, Phys. Rev. D **87** (2013) 054002.
- [47] U. Nierste, S. Trine, and S. Westhoff, Phys. Rev. D **78** (2008) 015006.
- [48] K. Kiers and A. Soni, Phys. Rev. D **56** (1997) 5786-5793.
- [49] M. Tanaka, Z. Phys. C **67** (1995) 321-326.
- [50] W.-S. Hou, Phys. Rev. D **48** (1993) 2342-2344.
- [51] H. N. Brown et al. [Muon g-2 Collaboration], Phys. Rev. Lett. **86** (2001) 2227.
- [52] G. W. Bennett et al. [Muon g-2 Collaboration], Phys. Rev. D **73** (2006) 072003.
- [53] F. Jegerlehner and A. Nyffeler, Phys. Rept. **477** (2009) 1.
- [54] G. Colangelo, M. Hoferichter, A. Nyffeler, M. Passera, and P. Stoffer, Phys. Lett. B **735** (2014) 90.
- [55] A. Kurz, T. Liu, P. Marquard, and M. Steinhauser, Phys. Lett. B **734** (2014) 144.
- [56] A. Dedes and H. E. Haber, JHEP **0105** (2001) 006.
- [57] K. M. Cheung, C. H. Chou and O. C. W. Kong, Phys. Rev. D **64** (2001) 111301.
- [58] F. Larios, G. Tavares-Velasco and C. P. Yuan, Phys. Rev. D **64** (2001) 055004.
- [59] K. Cheung and O. C. W. Kong, Phys. Rev. D **68** (2003) 053003.
- [60] J. Cao, P. Wan, L. Wu and J. M. Yang, Phys. Rev. D **80** (2009) 071701.
- [61] J. S. Lee and A. Pilaftsis, Phys. Rev. D **86** (2012) 035004.
- [62] M. Krawczyk, hep-ph/0103223.
- [63] A. Broggio, E. J. Chun, M. Passera, K. M. Patel and S. K. Vempati, JHEP **1411** (2014) 058.
- [64] L. Wang and X. F. Han, JHEP **05** (2015) 039.

- [65] T. Abe, R. Sato and K. Yagyu, arXiv:1504.07059.
- [66] E. J. Chun, Z. Kang, M. Takeuchi, Y.-L. Tsai, JHEP **1511** (2015) 099.
- [67] T. Han, S. K. Kang, J. Sayre, JHEP **1602** (2016) 097.
- [68] V. Ilisie, JHEP **1504** (2015) 077.
- [69] L. Wang, X.-F. Han, Phys. Rev. D **86** (2012) 095007.
- [70] A. Cherchiglia, P. Kneschke, D. Stockinger, H. Stockinger-Kim, arXiv:1607.06292.
- [71] X. Liu, L. Bian, X.-Q. Li, J. Shu, Nucl. Phys. B **909** (2016) 507-524.
- [72] X.-F. Han, L. Wang, J. M. Yang, Phys. Lett. B **757** (2016) 537-547.
- [73] R. A. Battye, G. D. Brawn, A. Pilaftsis, JHEP **1108** (2011) 020.
- [74] A. Pich, P. Tuzon, Phys. Rev. D **80** (2009) 091702.
- [75] V. Barger, L. L. Everett, H. E. Logan, and G. Shaughnessy, Phys. Rev. D **88** (2013) 115003.
- [76] T. P. Cheng and M. Sher, Phys. Rev. D **35** (1987) 3484.
- [77] J. Bernon, J. F. Gunion, H. E. Haber, Y. Jiang and S. Kraml, Phys. Rev. D **92** (2015) 075004.
- [78] P. S. Bhupal Dev, A. Pilaftsis, JHEP **12** (2014) 024.
- [79] D. Eriksson, J. Rathsman, O. Stål, Comput. Phys. Commun. **181** (2010) 189.
- [80] D. Eriksson, J. Rathsman, O. Stål, Comput. Phys. Commun. **181** (2010) 833.
- [81] B. Lautrup, A. Peterman, E. de Rafael, Phys. Rept. **3** (1972) 193-260.
- [82] J. P. Leveille, Nucl. Phys. B **137** (1978) 63.
- [83] D. Chang, W. S. Hou and W. Y. Keung, Phys. Rev. D **48** (1993) 217.
- [84] Y. Amhis et al. [Heavy Flavor Averaging Group (HFAG) Collaboration], arXiv:1412.7515.
- [85] C. Q. Geng and J. N. Ng, Phys. Rev. D **38** (1988) 2857 [Erratum-ibid. D **41**, 1715 (1990)].
- [86] M. Misiak, H. M. Asatrian, R. Boughezal, M. Czakon, T. Ewerth, A. Ferroglio, P. Fiedler, and P. Gambino et al., Phys. Rev. Lett. **114** (2015) 221801.
- [87] M. Ciuchini, G. Degrassi, P. Gambino and G. F. Giudice, Nucl. Phys. B **527** (1998) 21.
- [88] P. Bechtle, O. Brein, S. Heinemeyer, G. Weiglein, K. E. Williams, Comput. Phys. Commun. **181** (2010) 138.
- [89] P. Bechtle, O. Brein, S. Heinemeyer, O. Stål, T. Stefaniak, G. Weiglein, K. E. Williams, Eur. Phys. Jour. C **74** (2014) 2693.
- [90] ATLAS Collaboration, ATLAS-CONF-2016-088.
- [91] ATLAS Collaboration, ATLAS-CONF-2016-089.

- [92] ATLAS and CMX Collaborations, JHEP **1608** (2016) 045.
- [93] CMS Collaboration, Phys. Lett. B **736** (2014) 33.
- [94] G. Aad et al. [ATLAS Collaboration], JHEP **1510** (2015) 150.
- [95] J. Alwall, R. Frederix, S. Frixione, V. Hirschi, F. Maltoni, O. Mattelaer, H. -S. Shao, T. Stelzer, P. Torrielli, M. Zaro, JHEP **1407** (2014) 079.
- [96] A. Alloul, N. D. Christensen, C. Degrande, C. Duhr, B. Fuks, Comput. Phys. Commun. **185** (2014) 2250.
- [97] T. Sjostrand, S. Mrenna, P. Z. Skands, JHEP **0605** (2006) 026.
- [98] P. Golonka, B. Kersevan, T. Pierzchala, E. Richter-Was, Z. Was, M. Worek, Comput. Phys. Commun. **174** (2006) 818.
- [99] J. de Favereau, *et al.*, JHEP **1402** (2014) 057.
- [100] M. Cacciari, G. P. Salam, G. Soyez, Eur. Phys. Jour. C **72** (2012) 1896.
- [101] M. Cacciari, G. P. Salam, G. Soyez, JHEP **0804** (2008) 063.
- [102] M. Aaboud et al. [ATLAS Collaboration], arXiv:1608.00890.
- [103] X. Chen, L. Xia, Phys. Rev. D **93** (2016) 113010.
- [104] A. Elagin, P. Murat, A. Pranko, A. Safonov, Nucl. Instrum. Meth. A **654** (2011) 481.
- [105] G. Aad et al. [ATLAS Collaboration], Eur. Phys. Jour. C **76** (2016) 12.